European Journal of Radiology 178 (2024) 111614

Contents lists available at ScienceDirect

European Journal of Radiology

journal homepage: www.elsevier.com/locate/ejrad

Potential of non-contrast spiral breast CT to exploit lesion density and favor breast cancer detection: A pilot study

Julia Weber [a], Giulia Zanetti [a], Elizabet Nikolova [a], Thomas Frauenfelder [a], Andreas Boss [a,b], Jann Wieler [a,1], Magda Marcon [a,c,1,*]

[a] Diagnostic and Interventional Radiology, University Hospital Zurich, University of Zurich, Rämistrasse 100, 8091 Zurich, Switzerland
[b] GZO AG Spital Wetzikon, Spitalstrasse 66, Wetzikon 8620, Switzerland
[c] Institute of Radiology, Spital Lachen, Oberdorfstrasse 41, Lachen 8853, Switzerland

ARTICLE INFO

Keywords:
Breast neoplasm
Malignant breast lesion
Breast CT
Breast density

ABSTRACT

Purpose: To assess the density values of breast lesions and breast tissue using non-contrast spiral breast CT (nc-SBCT) imaging.
Method: In this prospective study women undergoing nc-SBCT between April-October 2023 for any purpose were included in case of: histologically proven malignant lesion (ML); fibroadenoma (FA) with histologic confirmation or stability > 24 months (retrospectively); cysts with ultrasound correlation; and women with extremely dense breast (EDB) and no sonographic findings. Three regions of interest were placed on each lesion and 3 different area of EDB. The evaluation was performed by two readers (R1 and R2). Kruskal-Wallis test, intraclass correlation (ICC) and ROC analysis were used.
Results: 40 women with 12 ML, 10 FA, 15 cysts and 9 with EDB were included. Median density values and interquartile ranges for R1 and R2 were: 60.2 (53.3–67.3) and 62.5 (55.67–76.3) HU for ML; 46.3 (41.9–59.5) and 44.5 (40.5–59.8) HU for FA; 35.3 (24.3–46.0) and 39.7 (26.7–52.0) HU for cysts; and 28.7 (24.2–33.0) and 33.3 (31.7–36.8) HU for EDB. For both readers, densities were significantly different for ML versus EDB ($p < 0.001$) and cysts ($p < 0.001$) and for FA versus EDB ($p=/<0.003$). The AUC was 0.925 (95 %CI 0.858–0.993) for R1 and 0.942 (0.884–1.00) for R2 when comparing ML versus others and 0.792 (0.596–0.987) and 0.833 (0.659–1) when comparing ML versus FA. The ICC showed an almost perfect inter-reader (0.978) and intra-reader agreement (>0.879 for both readers).
Conclusions: In nc-SBCT malignant lesions have higher density values compared to normal tissue and measurements of density values are reproducible between different readers.

1. Introduction

Despite the improvements achieved in breast cancer mortality over the last 30 years thanks to mammographic screening and effective treatments, breast cancer remains the most common cancer type worldwide in women and a leading cause of death in the female society [1]. The individual risk to develop breast cancer is determined by multiple factors, including family history and hormonal influence. Mammographic density, corresponding to the fraction of radiopaque fibro-glandular tissue compared to radiolucent adipose tissue in the breast also plays an important role for developing breast cancer: women with dense breast have a 2–6-fold increase of breast cancer in comparison to women with low dense breast tissue. Moreover, due to the masking effect, mammography sensitivity drops from 87-98 % to 30–63 % in case of women with extremely dense breasts [2]. Therefore, alternative screening modalities are sought to overcome these limitations of mammography.

Digital breast tomosynthesis (DBT) is a pseudo-3-D imaging

Abbreviations: ACR, American College of Radiology; BCT, breast computed tomography; CBBCT, cone-beam breast computed tomography; CEM, contrast enhanced mammography; DBT, digital breast tomosynthesis; EDB, extremely dense breast; FA, fibroadenoma; ML, malignant lesion; SBCT, spiral breast computed tomography; nc-SBCT, non-contrast spiral breast computed tomography.

* Corresponding author at: Diagnostic and Interventional Radiology, University Hospital Zurich, University of Zurich, Rämistrasse 100, 8091 Zurich, Switzerland.
E-mail address: magda.marcon@usz.ch (M. Marcon).

[1] Equal contribution.

https://doi.org/10.1016/j.ejrad.2024.111614
Received 11 February 2024; Received in revised form 30 June 2024; Accepted 10 July 2024
Available online 14 July 2024

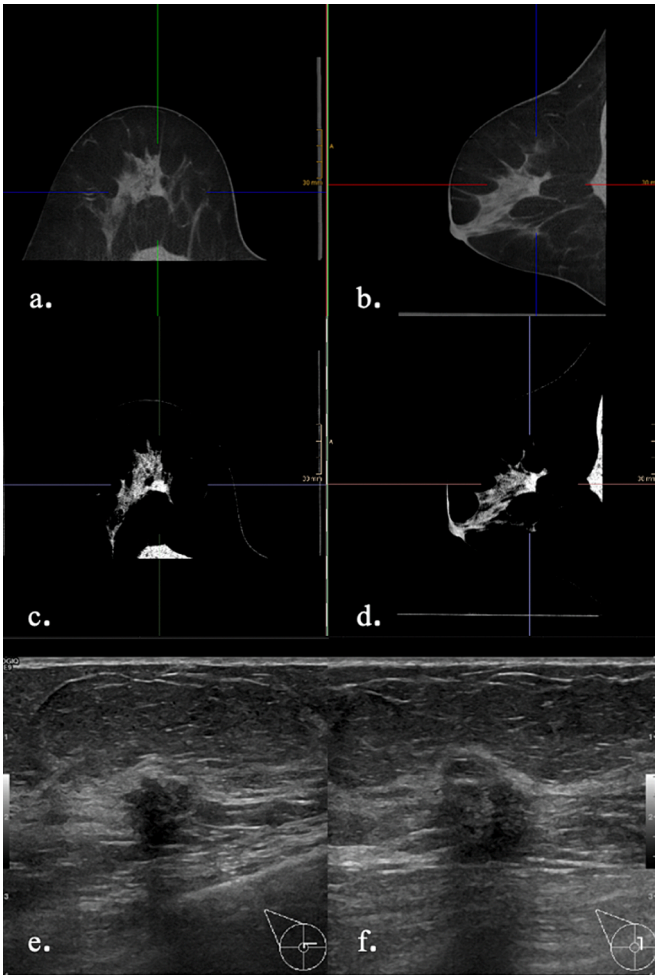

Fig. 1. 59-year-old woman undergoing nc-BCT for screening. The coronal (a) and sagittal (b) BCT images with the standard windowing and the corresponding axial (c) and sagittal (d) image after windowing to enhance lesion contrast are presented. A lesion can be identified at the 2o'clock position in the right breast. Mean density value measured by Reader 1 was 68.7 HU and by Reader 2 was 79.7 HU. In the ultrasound examination (e and f), a suspicious mass up to 9 mm could be identified at 2o'clock position in the same breast. US-guided biopsy was performed and the mass corresponded to an invasive ductal carcinoma.

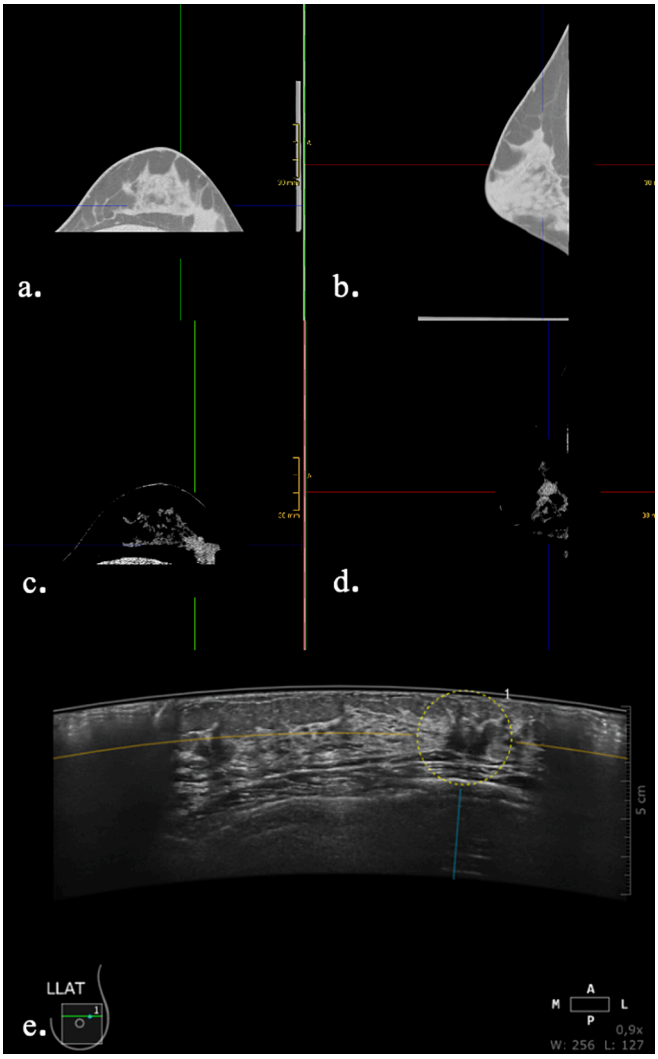

Fig. 2. 51-year-old woman undergoing nc-BCT for screening. The coronal (a) and sagittal (b) BCT images with the standard windowing and the corresponding axial (c) and sagittal (d) image after windowing to enhance lesion contrast are presented. A lesion can be identified at the 2o'clock position in the left breast. Mean density value measured by Reader 1 was 46.0 HU and by Reader 2 was 48.7 HU. In the ultrasound examination performed with an automated breast ultrasound system (e), a suspicious mass up to 10 mm could be identified at 2o'clock position in the same breast. US-guided biopsy was performed and the mass corresponded to an invasive ductal carcinoma.

technique that has the potential to reduce the masking effect and resolve superimposition of dense breast tissue. DBT has been investigated as an alternative for digital breast mammography. Recent studies have shown that DBT has higher sensitivity (up to 40 % increase compared to mammography) for breast cancer in all density categories and especially in women with highest breast density at the cost of slightly lower specificity and higher radiation dose [3]. Concerns regarding the use of DBT for screening are related to the risk of false-positives and overdiagnosis and results on the effect on the interval cancer rate are still mixed [4–6].

Use of supplemental breast ultrasound screening, performed with handheld or automated systems, can also increase cancer detection in women with dense breast; the drawbacks are the increase of recall and biopsy rates [7,8].

Contrast-enhanced breast MRI is the most sensitive imaging method for breast cancer detection. Recently, the Dutch DENSE trial and the international EA1411 ECOG-ACRIN study, focusing on breast screening with contrast-enhanced breast MRI in women with extremely dense breast could demonstrate that MRI screening can cost-effectively reduce mortality for breast cancer in this category of women [9–11]. In recent years, contrast enhanced mammography (CEM) has been introduced as a potential alternative to contrast enhanced MRI with lower costs and the same effectivity on providing functional information. So far, CEM has primarily been used in the diagnostic setting. Initial studies investigating the use of CEM in breast cancer screening have shown that CEM has superior performance compared with mammography and also mammography and supplemental ultrasound in women with dense breasts [12]. The main drawbacks concerning the use of breast MRI and CEM for screening remain the use of contrast medium, their limited availability, the long examination times and costs.

Dedicated Breast CT (BCT) systems have also been recently introduced in the market and the two commercially available systems are the cone-beam breast CT (CBBCT) and the more recently developed spiral breast CT (SBCT) using photon-counting detectors. These systems have shown potential as an alternative screening tool especially in women who refuse mammography examination because of pain due to breast compression. Indeed, during the examination the patient lies on the examination table in prone position and the breast is positioned in the

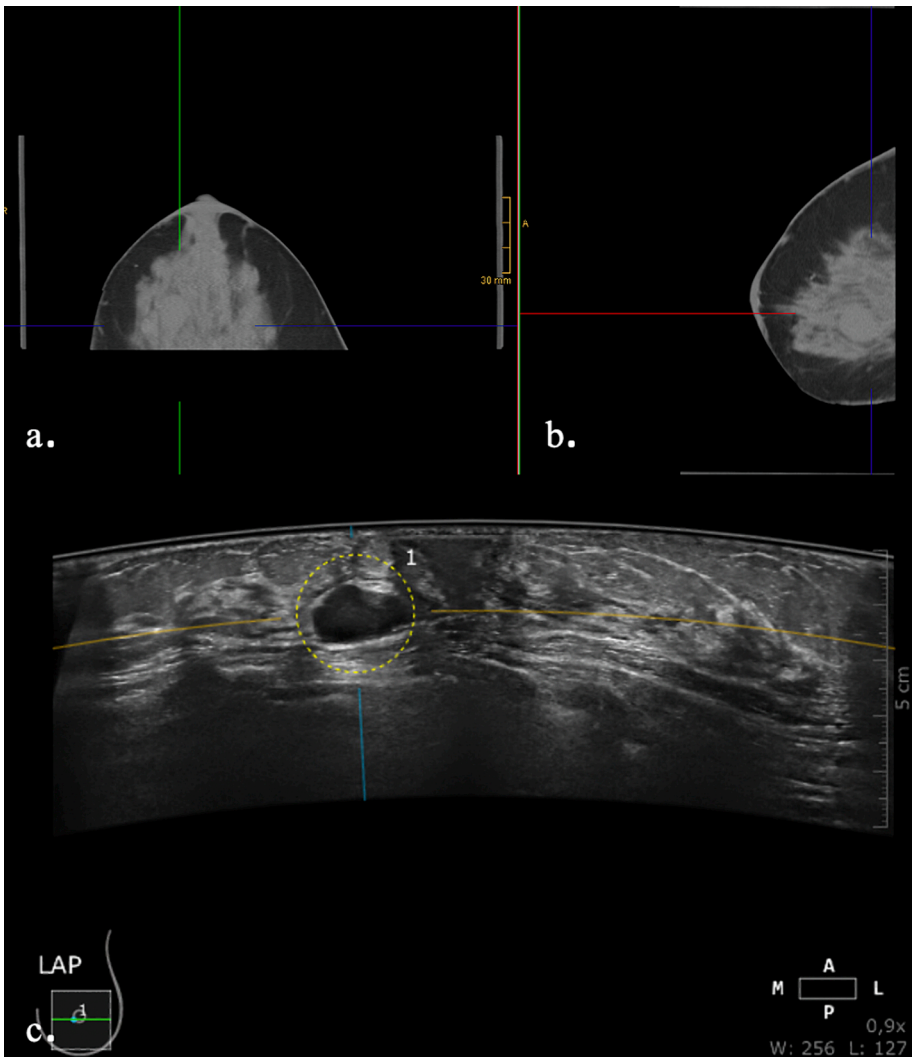

Fig. 3. 51 −year-old woman undergoing nc-BCT for screening. The coronal (a) and sagittal (b) BCT images are presented. A lesion can be identified at the 9o'clock position in the periareolar region of the left breast. Mean density value measured by Reader 1 was 44.3 HU and by Reader 2 was 43.3 HU. In the ultrasound examination performed with an automated breast ultrasound system (e), a cystic lesion up to 15 mm could be identified in the same position.

Table 1
Indications to perform nc-BCT among the different patients.

	Malignant lesions (n = 12)	**Fibroadenomas** (n = 8)	**Cysts** (n = 12)	**Glandular tissue** (n = 9)
Indication				
Screening (n = 30)	6 (50)	7 (87.5)	8 (66.7)	9 (100)
Follow-up after breast cancer (n = 1)	0 (0)	0 (0)	1 (8.3)	0 (0)
Palpable mass (n = 8)	6 (50)	0 (0)	2 (16.7)	0 (0)
Mastodynia (n = 1)	0 (0)	1 (12.5)	0 (0)	0 (0)
Second look after breast MRI (n = 1)	0 (0)	0 (0)	1 (8.3)	0 (0)

Table 2
Malignant lesions features.

	nc-BCT maximum diameter (mm)	Calcifications	Histologic diagnosis
1	16	Yes	IDC and ILC
2	27	No	IDC
3	17	No	IDC
4	14	No	IDC
5	27	No	IDC
6	10	No	IDC
7	9	No	IDC
8	18	Yes	IDC
9	25	No	IDC
10	30	Yes	IDC
11	10	No	IDC
12	22	No	IDC

IDC, invasive ductal carcinoma; *ILC*, invasive lobular carcinoma.

center of a table hole [13]. SBCT provides fully 3D imaging and therefore, by eliminating tissue overlap, could increase lesion detection [14–18]. Moreover, lesion density can be objectively measured. The Hounsfield Unit (HU) is routinely used for the interpretation of CT images and for quantitively measure a tissue radiodensity (depending on the tissue absorption/attenuation of the X-ray beam) with air arbitrarily defined as −1000 HU and water as 0 (zero) HU. Benign and malignant breast lesions exhibit different densities and previous mammography studies have shown that the density of a mass correlates with the degree of malignancy [19,20]. Nevertheless, evaluation of lesion density in

Table 3
Median density values and interquartile ranges (in parenthesis) for the two readers and different tissue categories, intra-reader agreement and p-value from the comparison of density measurements. HU=Hounsfield unit.

	Tissue category and median density value (HU) (IQR)	Intra-reader agreement – ICC (95 % C.I.)		p-value
Reader 1	Malignant lesions		Fibroadenoma	0.147
	60.2	0.998	Cysts	0.00009*
	(53.3–67.3)	(0.994–0999)	Glandular tissue	<0.00001*
	Fibroadenoma		Cysts	0.029*
	44.5	0.956	Glandular	0.001*
	(40.5—59.8)	(0.870–0.988)	tissue	
	Cysts		Glandular	0.288
	35.3	0.982	tissue	
	(24.3—46.0)	(0.958–0.994)		
	Glandular tissue			
	28.7	0.903		
	(24.2—33.0)	(0.696–0.976)		
Reader 2	Malignant lesion		Fibroadenoma	0.063
	62.5	0.997	Cysts	0.0002*
	(55.67–76.3)	(0.991–0.999)	Glandular tissue	<0.00001*
	Fibroadenoma		Cysts	0.110
	44.5	0.989	Glandular	0.003*
	(40.5—59.8)	(0.969–0.997)	tissue	
	Cysts		Glandular	0.132
	39.7	0.996	tissue	
	(26.7—52.0)	(0.991–0.999)		
	Glandular tissue			
	33.3	0.879		
	(31.7–36.8)	(0.621–0.970)		

*Difference is statistically significant.
IQR, interquartile range.

mammography is based on a qualitative evaluation and its accuracy is hampered by reader experience and subjectivity. BCT imaging offers the possibility to quantify density differences.

The purpose of our study is to investigate the density differences between breast lesions and breast glandular tissue in non-contrast SBCT (nc-SBCT).

2. Method

2.1. Patient selection

This prospective study was approved by the local ethics committee (BASEC 2018–01694, DRKS00015475). Each patient undergoing SBCT gave a written informed consent. Between April 2023 and October 2023, a total of 640 nc-SBCT examinations were performed. Nc-SBCT is offered as an alternative to mammography to all women who prefer not to undergo breast compression during mammography examination and indications include: screening, follow-up after breast conserving surgery, palpable lump and mastodynia and second-look after breast-MRI. supplemental breast ultrasound is additionally performed for all cases with dense breast, SBCT unclear findings and lack of clinical-imaging correlation. A breast imaging fellow recorded consecutive cases with: (a) extremely dense breast tissue on BCT as annotated in the clinical report and evaluated according to a previous publication [21] (b) histologically proven breast cancer visible in nc-SBCT as a mass with/without intralesional calcifications (c) known fibroadenomas clearly visible in nc-SBCT with a diameter of at least 1 cm and that either had a stable follow up of at least 2 years or were histologically proven (d) cysts with clear sonographic correlation. Cases with lesions marked with biopsy clips and cases of breast cancer only visible as microcalcifications and no mass on nc-SBCT were excluded. Information regarding indication to perform nc-BCT, histology of the lesion, lesion maximum diameter and lesion position were annotated.

2.2. CT-Imaging protocol and image reading

All examinations were performed with a SBCT (nu:view, AB CT-Advanced Breast-CT GmbH, Erlangen, Germany). The scanning protocol includes one scan per breast without contrast medium injection, including an adapted scan length (80, 120, 160 mm), with a fixed tube voltage of 60 kV and a tube current of 25 mA. Raw image data are routinely reconstructed to 0.3 mm axial slices for soft tissue evaluation (ST-reconstruction) and to 0.15 mm axial slices for microcalcification evaluation (HR-reconstruction). The total number of slices per breast acquired in the axial plane varied between 313 and 589 for the ST-reconstruction and between 626 and 1179 for the HR-reconstruction. The examinations were analyzed in the same standardized manner: first the HR-reconstruction in 15 mm MIP axial and sagittal reformation using a bone window thus facilitating the detection and characterization of the distribution of calcifications. Second the ST-reconstruction in 3 mm averaged axial and sagittal reformation using a soft tissue window to detect asymmetries, architectural distortions and soft tissue lesions.

2.3. Image analysis

Two readers with different level of experience in breast imaging independently performed the analysis (Reader 1, three months experience and Reader 2, with more than 5 years), placing regions of interest (ROI) in index lesions and in the glandular tissue. Readers were informed about the position of the target lesion but not about the histology. For each reader, three representative density values were obtained from each lesion by placing three circular ROIs as large as possible within the margins of the lesions at three different levels. ROI diameter, mean density (expressed as HU), and standard deviation values were annotated for each measure. For the evaluation of the glandular tissue density a ROI with a defined diameter of 1 cm was placed in three different regions of each breast avoiding area with visible fat tissue. Image analysis was performed on a PACS workstation equipped with a dedicated breast imaging display software (DeepUnity, Dedalus).

2.4. Statistical analysis

Variables are presented as mean ± standard deviation if normally distributed and as median and interquartile range (IQR) if non-normally distributed. Kruskal-Wallis test was used to compare density values among different tissue categories (i.e. malignant lesions, fibroadenomas, cysts, glandular tissue) and the Mann-Whitney-*U* test to compare density between malignant lesions with and without calcifications. The data were graphically represented using Bland-Altman plots. The inter-reader agreement for the different tissue density measurements and intra-reader agreement for the density measurements in the same lesion or in the same breast for the glandular tissue measurements were evaluated using the intraclass correlation coefficient (ICC) and interpreted according to the Landis and Koch (with 0.00–0.20 indicating slight agreement, 0.21–0.40 fair agreement, 0.41–0.60 moderate agreement, 0.61–0.80 substantial agreement and 0.81–1.00 almost perfect agreement) [22]. Paired *t*-test was used to compare mean ROI diameter between the two readers. The effectiveness of the density value in distinguishing malignant from benign lesions and normal tissue as well as in distinguishing malignant lesions from fibroadenomas was evaluated by using receiver operating characteristics (ROC) analysis. The optimal thresholds for differentiating malignant lesions from benign lesions and normal tissue and malignant lesions from fibroadenomas were chosen at the highest possible sensitivity and specificity on the ROC curves. Statistics were performed by using SPSS software (SPSS, version 22.0; SPSS) and $p < 0.05$ was considered to indicate statistical significance.

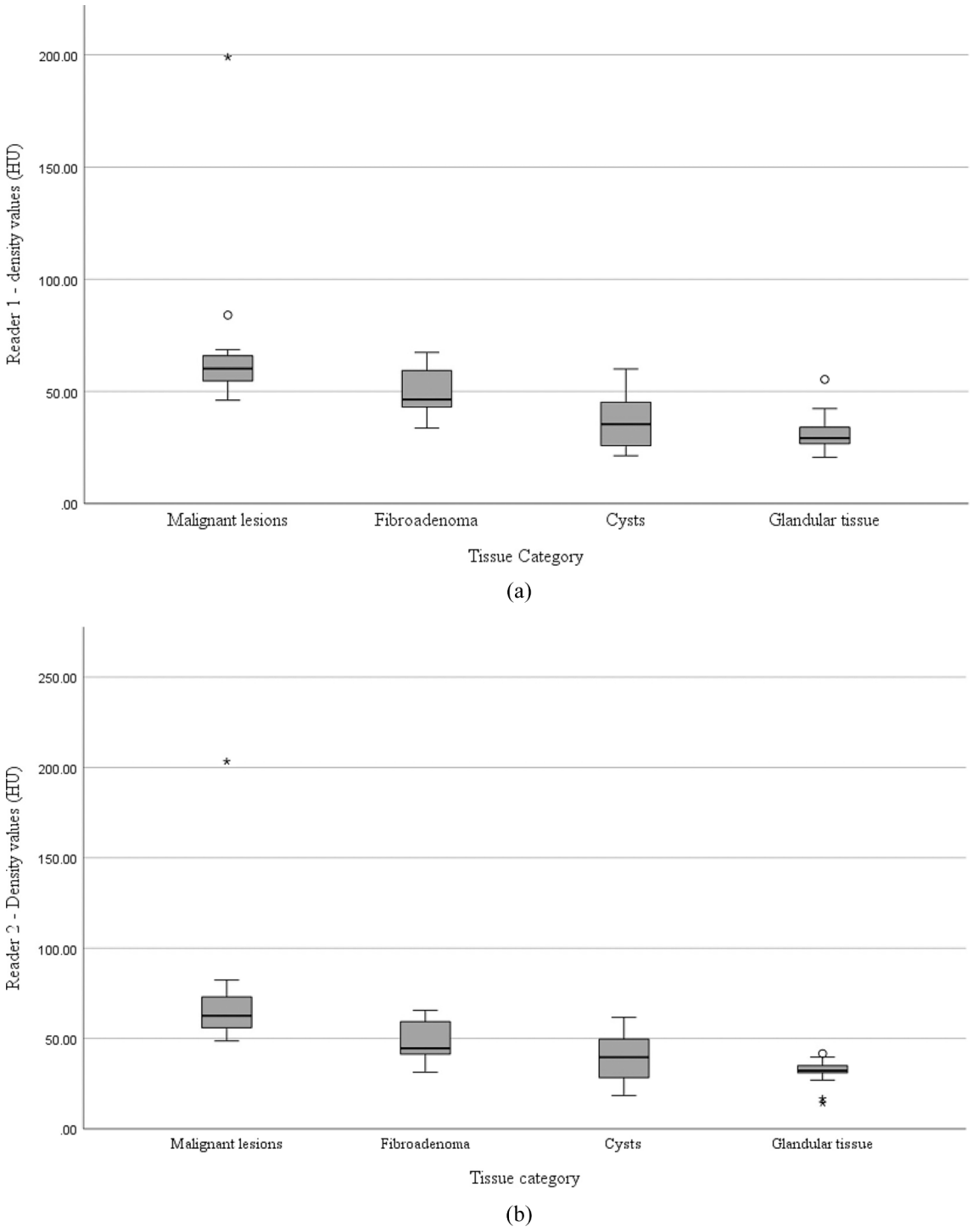

Fig. 4. Box plots show comparison of the density values measured on the different tissue categories by Reader 1 (a) and 2 (b). The line within the box represents the median value. Boxes represent 25th to 75th percentiles. The lines outside indicate the 10th and 90th percentiles.

3. Results

A total of 40 women were included in the study: 12 patients with a malignant lesions (median age 56.5 years, 51.2–72.0); 7 women with fibroadenomas (51.0 years, 49.5–59.5), one of them with 3 lesions; 12 patients with cysts (51.0 years, 48.5—52.5), 3 of them with 2 lesions; and 9 women with extremely dense glandular tissue and no findings on nc-SBCT or ultrasound (51.0 years, 45.0 – 55.0) (Figs.1–3). Indications to perform nc-SBCT are reported in Table 1.

A total of 12 malignant lesions (median diameter 17.5 mm, IQR 11.0–26.5 mm), 10 fibroadenoma (median diameter 10 mm, IQR 10–17.8 mm) and 15 cysts (median diameter 15 mm, IQR 12–21 mm) were included. For all malignant lesions, detailed information is reported in Table 2. Three malignant lesions also contained microcalcifications. None of the benign lesions contained calcifications.

Mean ROI diameter for Reader 1 was 7.4 ± 2.6 mm, 6.2 ± 2.0 mm and 7.3 ± 2.5 mm for malignant lesions, fibroadenomas and cysts, respectively. For Reader 2, mean ROI diameter was 8.2 ± 3.5 mm, 7.0 ± 2.8 mm and 10.0 ± 4.5 mm, for malignant lesions, fibroadenomas and cysts, respectively. The mean ROI diameter was significantly different

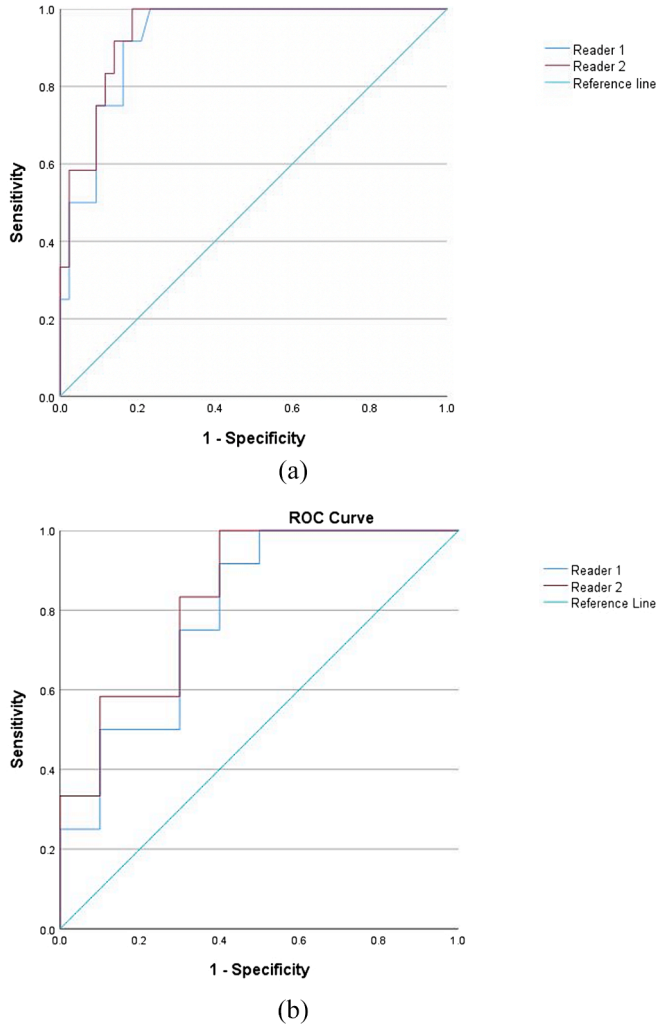

Fig. 5. (a) ROC-Curve for the density value for differentiating malignant lesions from fibroadenomas, cysts and glandular tissue for Reader 1 and Reader 2. The AUC is 0.925 (95% C.I.: 0.86–0.99) for Reader 1 and 0.942 (95% C.I. 0.88–1.00) for Reader 2. (b) ROC-Curve for the density value for differentiating malignant lesions from fibroadenomas for Reader 1 and Reader 2. The AUC is 0.792 (95% C.I. 0.596–0.987) for Reader 1 and 0.833 (95% C.I. 0.659–1) for Reader 2.

for all lesion analysis: malignant lesions ($p = 0.012$), cysts ($p < 0.001$) and fibroadenomas ($p = 0.012$).

Table 3 and Fig. 4 summarize median density values for the two readers for malignant lesions, fibroadenomas, cysts and glandular tissue. For Reader 1, a significantly higher density was found for malignant lesions compared to the glandular tissue ($p < 0.001$), malignant lesions compared to cysts ($p < 0.001$) and fibroadenomas compared to the glandular tissue ($p = 0.001$) and to cysts ($p = 0.029$). Among the other categories no significant differences were found ($p > 0.147$). For Reader 2, a significantly higher density was found for malignant lesions compared to the glandular tissue ($p < 0.001$), malignant lesions compared to cysts ($p < 0.001$) and fibroadenomas compared to the glandular tissue ($p = 0.003$) but no significant differences were found among the other categories ($p > 0.063$). No significant difference was found for density values of malignant lesions with or without associated microcalcifications ($p = 0.145$ for both Readers).

The AUC for the ROC analysis was 0.925 (95 % C.I.: 0.858–0.993) for Reader 1 and 0.942 (95 % C.I.: 0.884–1) for Reader 2 when comparing density values of malignant lesions versus fibroadenoma, cysts and normal glandular tissue (Fig. 5a). For Reader 1, using a cut-off value of 45.7 HU resulted in a sensitivity of 100 % with a specificity of 76.7 % whereas utilizing a cut-off value of 46.3 HU yielded a sensitivity of 91.7 % and specificity 79.4 %; for Reader 2, the use of a threshold value of 48.0 HU led to a sensitivity of 100 % with a specificity of 81.4 % while using a cut-off value of 50.3 HU resulted in a sensitivity of 91.7 % and specificity 81.4 %. When comparing density values of malignant lesions and fibroadenoma the AUC was 0.792 (95 % C.I.: 0.596–0.987) for Reader 1 and 0.833 (95 % C.I.: 0.659–1) for Reader 2 (Fig. 5b). For Reader 1, using a cut-off value of 56.2 HU resulted in a sensitivity of 75.0 % with a specificity of 70.0 %; similarly, for Reader 2, the use of a threshold value of 56.0 HU led to a sensitivity of 75.0 % with a specificity of 70.0 %.

The ICC showed an almost perfect inter-reader agreement in the density measures of the targeted lesions and tissue (0.978, 95 % C.I.: 0.961–0.988). Bland-Altman plot for inter-reader agreement showed rather narrow limits; no systematic bias was present between observers for density evaluation ($p = 0.587$) (Fig. 6).

For Reader 1, ICC showed an almost perfect intra-reader agreement when measuring malignant lesions (0.998, 95 % C.I.: 0.994–0.999), fibroadenomas (0.956, 95 % C.I.: 0.870–0.988), cysts (0.982, 95 % C.I.: 0.958–0.994) and glandular tissue (0.903, 95 % C.I.: 0.696–0.976). Similarly for Reader 2 ICC showed an almost perfect intra-reader agreement for all categories: malignant lesions (0.997, 95 % C.I.: 0.991–0.999), fibroadenomas (0.989, 95 % C.I.: 0.969–0.997), cysts (0.996, 95 % C.I.: 0.991–0.999) and glandular tissue (0.879, 95 % C.I.: 0.621–0.970) (Table 3).

4. Discussion

In our study malignant lesions in nc-SBCT exhibited significant higher density values in comparison with dense glandular tissue and with cystic lesions whereas similar density values were found between malignant lesions and fibroadenomas.

So far, most published studies investigating the use of SBCT, have highlighted its advantages in terms of increased patient comfort and reduced compression related-pain, especially in premenopausal women [18,23,24]. Although prospective clinical trials applying BCT for screening in big populations are still missing, due to the possibility to reduce tissue overlay similar to DBT, it can be expected that higher sensitivity may be achieved particularly in case of intermediate breast density category (ACR category B or C) [25]. Nevertheless, in case of extremely dense breast (ACR category D), lesion detection based on morphological features i.e. shape and margin could remain challenging. The possibility to measure the density on each slice and therefore to quantify the difference in density of malignant lesions compared to glandular breast tissue and benign lesions may offer a unique opportunity for lesion detection and more objective characterization without contrast medium administration also in women with extremely dense breast. This, together with reduced scan time, would represent a major advantage compared to breast-MRI and CEM, where use of contrast medium remains mandatory for lesion detection and long acquisition time are still required and also to supplemental breast ultrasound which is still hampered by the operator dependence, limited reproducibility and long acquisition time [9,12,24]. A direct comparison between SBCT and MRI/CEM regarding lesion detection does not exist to our knowledge.

Using a cut-off density value between 45 HU and 50 HU high sensitivity as well as specificity can be achieved for malignant lesions categorization compared to other breast tissue categories, excepted fibroadenomas. Moreover, no significant difference was found between cyst and glandular tissue density, offering the potential advantage to reduce the number of recalls for benign findings after screening with SBCT. The differentiation of malignant lesions from fibroadenomas remains more challenging with AUC of 0.792 and 0.833 for the two readers. At the best of our knowledge, only a recent study has investigated the density measurements in BCT for lesion characterization,

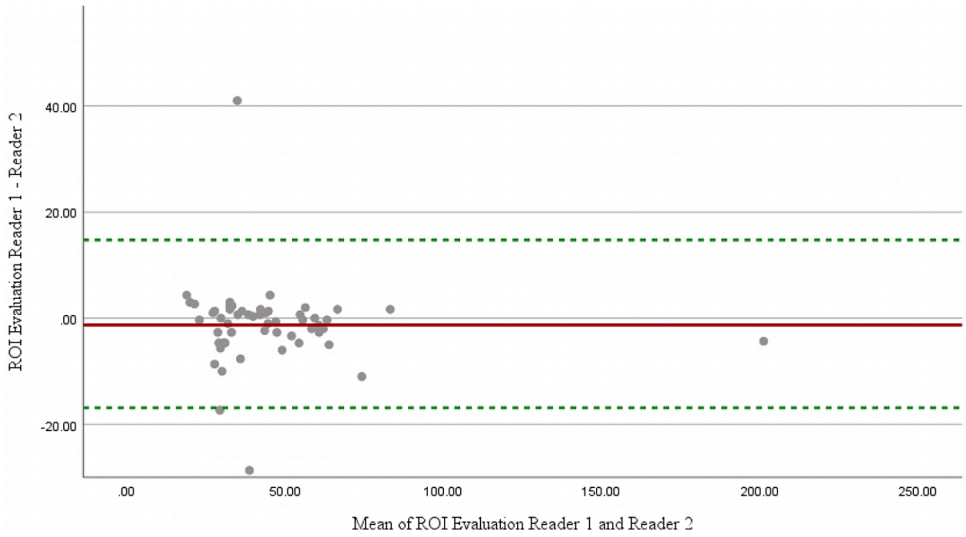

Fig. 6. Bland-Altman plot evaluating inter-reader agreement for density values measured by the two readers. The solid line represents the mean absolute difference; the dashed lines represent 95% limits of agreement.

using a different BCT system based on the cone-beam technology [26]. Density values were directly measured on the lesion and after normalization with fat and glandular tissue values, showing no difference between the three methods. Moreover, similarly to our results, no significant difference was found in non-enhanced scan when comparing density of malignant and solid benign lesions, although including not only fibroadenoma but also benign lobular tumor, breast hyperplasia, inflammatory changes and lipoma, with reported density values of 76.2 HU±67.9 and 83.6 HU±53.2, respectively. Higher density values for malignant compared to benign lesions have been shown after contrast-media administration. A more limited range of density values in our subcategories may be explained by the inclusion of only fibroadenomas in the solid benign lesion group but also by the fixed tube parameter during the acquisition (tube voltage of 60 kV and a tube current of 25 mA) whereas with the cone-beam BCT the tube current is automatically adjusted according to the size and density of patient's glandular tissue [27]. Moreover, analysis of inter-reader as well as intra-reader agreement has shown high reproducibility of the lesion measurements regardless of lesion category, lesion size and ROI size. This is an important finding because low reproducibility of lesion measurements limits its application. For example, use of ADC measurements in breast-MRI would be beneficial for lesion characterization but still its use remains limited because of a lack of standardization and also inter-reader variation [28]. Although our results should be confirmed by similar measurements performed with the same system in other institutions, we expect that similar density values could be obtained using the same tube parameters.

Due to the high amount of images obtained with SBCT examination, image evaluation could be time expensive and the risk exists that small lesions can be overviewed. Moreover, the use of a different windowing could facilitate or limit the lesion identification. Artificial intelligence tools for breast density classification and calcification detection have already proved feasibility and future investigation should focus on their application also for detection of lesions in non-contrast SBCT [29,30].

The study has some limitations. First, the number of cases included is small. Nevertheless, this was a preliminary study to prove the feasibility on differentiation of breast lesions and more extensive studies will follow to support our findings. Second, glandular tissue values were evaluated only in case of extremely dense breast tissue assuming that in women with lower representation of glandular tissue, density values should be lower and differences with breast lesions even more evident. Third, the readers were informed about the position of the lesion that facilitate its identification; however, the purpose of the study was to investigate lesion density values and not lesion detection. Third, the smaller malignant lesions had a maximum diameter of 9 mm and it is unclear if also smaller lesion could be identified and have similar density values or if measurements could be affected by some image noise.

In conclusion, in nc-SBCT malignant lesions have higher density values compared to cystic lesions and normal tissue, which may result in a better detection of lesions even in high breast density. The measurements of density values are highly reproducible between different readers.

CRediT authorship contribution statement

Julia Weber: Writing – original draft, Investigation, Data curation. **Giulia Zanetti:** Writing – review & editing, Data curation. **Elizabet Nikolova:** Writing – review & editing, Data curation. **Thomas Frauenfelder:** Writing – review & editing, Supervision. **Andreas Boss:** Writing – review & editing, Supervision. **Jann Wieler:** Writing – review & editing, Writing – original draft, Supervision, Methodology, Investigation, Conceptualization. **Magda Marcon:** Writing – original draft, Supervision, Methodology, Formal analysis, Conceptualization.

Declaration of competing interest

The authors declare that they have no known competing financial interests or personal relationships that could have appeared to influence the work reported in this paper.

References

[1] P. Advani, A. Moreno-Aspitia, Current strategies for the prevention of breast cancer, Breast Cancer Dove Med. Press 6 (2014) 59–71, https://doi.org/10.2147/BCTT.S39114.
[2] P.E. Freer, Mammographic breast density: impact on breast cancer risk and implications for screening, Radiogr. Rev. Publ. Radiol. Soc. N. Am. Inc 35 (2015) 302–315. https://doi.org/10.1148/rg.352140106.
[3] W. Heindel, S. Weigel, J. Gerß, H.-W. Hense, A. Sommer, M. Krischke, L. Kerschke, TOSYMA Screening Trial Study Group, Digital breast tomosynthesis plus synthesised mammography versus digital screening mammography for the detection of invasive breast cancer (TOSYMA): a multicentre, open-label, randomised, controlled, superiority trial, Lancet Oncol. 23 (2022) 601–611, https://doi.org/10.1016/S1470-2045(22)00194-2.
[4] J. Olinder, K. Johnson, A. Åkesson, D. Förnvik, S. Zackrisson, Impact of breast density on diagnostic accuracy in digital breast tomosynthesis versus digital mammography: results from a European screening trial, Breast Cancer Res. BCR 25 (2023) 116, https://doi.org/10.1186/s13058-023-01712-6.

[5] K. Johnson, J. Olinder, A. Rosso, I. Andersson, K. Lång, S. Zackrisson, False-positive recalls in the prospective Malmö Breast Tomosynthesis Screening Trial, Eur. Radiol. 33 (2023) 8089–8099, https://doi.org/10.1007/s00330-023-09705-x.
[6] M.L. Marinovich, K.E. Hunter, P. Macaskill, N. Houssami, Breast Cancer Screening Using Tomosynthesis or Mammography: A Meta-analysis of Cancer Detection and Recall, J. Natl. Cancer Inst. 110 (2018) 942–949, https://doi.org/10.1093/jnci/djy121.
[7] A. Vourtsis, W.A. Berg, Breast density implications and supplemental screening, Eur. Radiol. 29 (2019) 1762–1777, https://doi.org/10.1007/s00330-018-5668-8.
[8] W.A. Berg, Z. Zhang, D. Lehrer, R.A. Jong, E.D. Pisano, R.G. Barr, M. Böhm-Vélez, M.C. Mahoney, W.P. Evans, L.H. Larsen, M.J. Morton, E.B. Mendelson, D.M. Farria, J.B. Cormack, H.S. Marques, A. Adams, N.M. Yeh, G. Gabrielli, ACRIN 6666 Investigators, Detection of breast cancer with addition of annual screening ultrasound or a single screening MRI to mammography in women with elevated breast cancer risk, JAMA 307 (2012) 1394–1404, https://doi.org/10.1001/jama.2012.388.
[9] R.M. Mann, A. Athanasiou, P.A.T. Baltzer, J. Camps-Herrero, P. Clauser, E. M. Fallenberg, G. Forrai, M.H. Fuchsjäger, T.H. Helbich, F. Killburn-Toppin, M. Lesaru, P. Panizza, F. Pediconi, R.M. Pijnappel, K. Pinker, F. Sardanelli, T. Sella, I. Thomassin-Naggara, S. Zackrisson, F.J. Gilbert, C.K. Kuhl, European Society of Breast Imaging (EUSOBI), Breast cancer screening in women with extremely dense breasts recommendations of the European Society of Breast Imaging (EUSOBI), Eur. Radiol. 32 (2022) 4036–4045, https://doi.org/10.1007/s00330-022-08617-6.
[10] C.E. Comstock, C. Gatsonis, G.M. Newstead, B.S. Snyder, I.F. Gareen, J.T. Bergin, H. Rahbar, J.S. Sung, C. Jacobs, J.A. Harvey, M.H. Nicholson, R.C. Ward, J. Holt, A. Prather, K.D. Miller, M.D. Schnall, C.K. Kuhl, Comparison of Abbreviated Breast MRI vs Digital Breast Tomosynthesis for Breast Cancer Detection Among Women With Dense Breasts Undergoing Screening, JAMA 323 (2020) 746–756, https://doi.org/10.1001/jama.2020.0572.
[11] S.G.A. Veenhuizen, S.V. de Lange, M.F. Bakker, R.M. Pijnappel, R.M. Mann, E. M. Monninkhof, M.J. Emaus, P.K. de Koekkoek-Doll, R.H.C. Bisschops, M.B. I. Lobbes, M.D.F. de Jong, K.M. Duvivier, J. Veltman, N. Karssemeijer, H.J. de Koning, P.J. van Diest, W.P.T.M. Mali, M.A.A.J. van den Bosch, C.H. van Gils, W. B. Veldhuis, DENSE Trial Study Group, Supplemental Breast MRI for Women with Extremely Dense Breasts: Results of the Second Screening Round of the DENSE Trial, Radiology 299 (2021) 278–286, https://doi.org/10.1148/radiol.2021203633.
[12] K. Coffey, M.S. Jochelson, Contrast-enhanced mammography in breast cancer screening, Eur. J. Radiol. 156 (2022) 110513, https://doi.org/10.1016/j.ejrad.2022.110513.
[13] M. Wetzl, M. Dietzel, S. Ohlmeyer, M. Uder, E. Wenkel, Spiral breast computed tomography with a photon-counting detector (SBCT): The future of breast imaging? Eur. J. Radiol. 157 (2022) 110605 https://doi.org/10.1016/j.ejrad.2022.110605.
[14] N. Berger, M. Marcon, N. Saltybaeva, W.A. Kalender, H. Alkadhi, T. Frauenfelder, A. Boss, Dedicated breast computed tomography with a photon-counting detector: initial results of clinical in vivo imaging, Invest. Radiol. 54 (2019) 409–418, https://doi.org/10.1097/RLI.0000000000000552.
[15] S. Wienbeck, J. Lotz, U. Fischer, Review of clinical studies and first clinical experiences with a commercially available cone-beam breast CT in Europe, Clin. Imaging 42 (2017) 50–59, https://doi.org/10.1016/j.clinimag.2016.11.011.
[16] N. Berger, M. Marcon, T. Frauenfelder, A. Boss, Dedicated spiral breast computed tomography with a single photon-counting detector: initial results of the first 300 women, Invest. Radiol. 55 (2020) 68–72, https://doi.org/10.1097/RLI.0000000000000609.
[17] C. Zellweger, N. Berger, J. Wieler, D. Cioni, E. Neri, A. Boss, T. Frauenfelder, M. Marcon, Breast computed tomography: diagnostic performance of the maximum intensity projection reformations as a stand-alone method for the detection and characterization of breast findings, Invest. Radiol. 57 (2022) 205–211, https://doi.org/10.1097/RLI.0000000000000829.
[18] C.S. Schmidt, C. Zellweger, J. Wieler, N. Berger, M. Marcon, T. Frauenfelder, A. Boss, Clinical assessment of image quality, usability and patient comfort in dedicated spiral breast computed tomography, Clin. Imaging 90 (2022) 50–58, https://doi.org/10.1016/j.clinimag.2022.07.001.
[19] R.W. Woods, G.S. Sisney, L.R. Salkowski, K. Shinki, Y. Lin, E.S. Burnside, The mammographic density of a mass is a significant predictor of breast cancer, Radiology 258 (2011) 417–425, https://doi.org/10.1148/radiol.10100328.
[20] R.W. Woods, L. Oliphant, K. Shinki, D. Page, J. Shavlik, E. Burnside, Validation of results from knowledge discovery: mass density as a predictor of breast cancer, J. Digit. Imaging 23 (2010) 554–561, https://doi.org/10.1007/s10278-009-9235-3.
[21] J. Wieler, N. Berger, T. Frauenfelder, M. Marcon, A. Boss, Breast density in dedicated breast computed tomography: Proposal of a classification system and interreader reliability, Medicine (baltimore) 100 (2021) e25844.
[22] J.R. Landis, G.G. Koch, The measurement of observer agreement for categorical data, Biometrics 33 (1977) 159–174.
[23] M. Wetzl, E. Wenkel, M. Dietzel, L. Siegler, J. Emons, E. Dethlefsen, F. Heindl, C. Kuhl, M. Uder, S. Ohlmeyer, Potential of spiral breast computed tomography to increase patient comfort compared to DM, Eur. J. Radiol. 145 (2021) 110038, https://doi.org/10.1016/j.ejrad.2021.110038.
[24] H. Li, L. Yin, N. He, P. Han, Y. Zhu, Y. Ma, A. Liu, H. Lu, Z. Gao, P. Liu, Y. Wu, Z. Ye, Comparison of comfort between cone beam breast computed tomography and digital mammography, Eur. J. Radiol. 120 (2019) 108674, https://doi.org/10.1016/j.ejrad.2019.108674.
[25] Quelle: D'Orsi CJ, Sickles EA, Mendelson EB, Morris EA, et al., Atlas, Breast Imaging Reporting and Data System. Reston, VA, American College of Radiology, (2013).
[26] W. Wei, X.L. Yi, J. Yang, H. Liao, D. Su, CT values of contrast-enhanced CBBCT: A useful diagnostic tool for benign and malignant breast lesions, Acta Radiol. Stockh. Swed. 1987 (64) (2023) 2379–2386, https://doi.org/10.1177/02841851231177379.
[27] Y. Zhu, A.M. O'Connell, Y. Ma, A. Liu, H. Li, Y. Zhang, X. Zhang, Z. Ye, Dedicated breast CT: state of the art-Part I. Historical evolution and technical aspects, Eur. Radiol. 32 (2022) 1579–1589, https://doi.org/10.1007/s00330-021-08179-z.
[28] H. Bickel, P. Clauser, K. Pinker, T. Helbich, I. Biondic, B. Brkljacic, M. Dietzel, G. Ivanac, B. Krug, M. Moschetta, V. Neuhaus, K. Preidler, P. Baltzer, Introduction of a breast apparent diffusion coefficient category system (ADC-B) derived from a large multicenter MRI database, Eur. Radiol. 33 (2023) 5400–5410, https://doi.org/10.1007/s00330-023-09675-0.
[29] A. Landsmann, C. Ruppert, J. Wieler, P. Hejduk, A. Ciritsis, K. Borkowski, M. C. Wurnig, C. Rossi, A. Boss, Radiomics in photon-counting dedicated breast CT: potential of texture analysis for breast density classification, Eur. Radiol. Exp. 6 (2022) 30, https://doi.org/10.1186/s41747-022-00285-x.
[30] A. Landsmann, C. Ruppert, K. Borkowski, P. Hejduk, A. Ciritsis, J. Wieler, C. Rossi, A. Boss, Detection of microcalcifications in photon-counting dedicated breast-CT using a deep convolutional neural network: Proof of principle, Clin. Imaging 95 (2023) 28–36, https://doi.org/10.1016/j.clinimag.2022.12.006.